Volume 2 | Number 48 | 28 December 2014 | Pages 10221–10478

Journal of Materials Chemistry C

Materials for optical, magnetic and electronic devices

www.rsc.org/MaterialsC

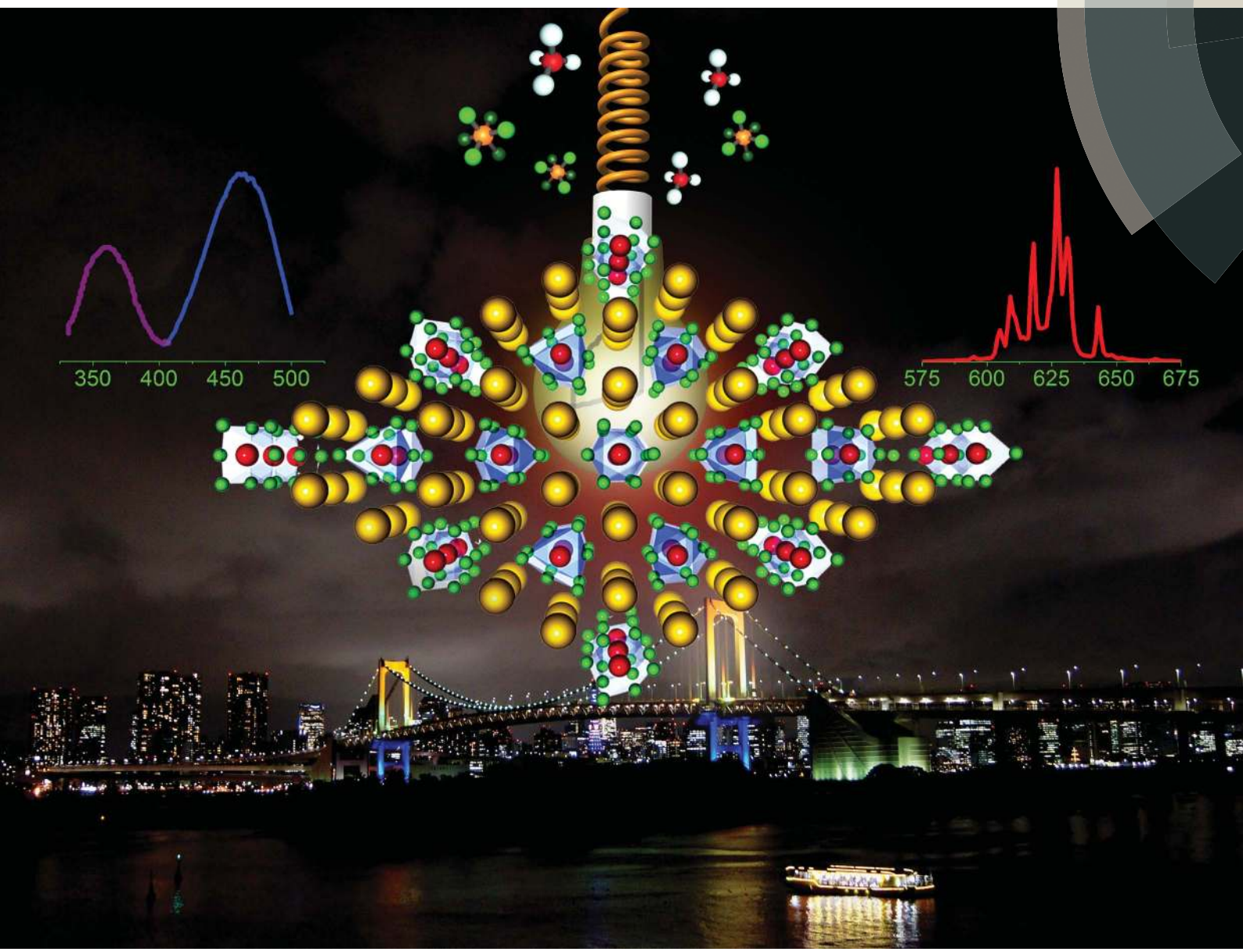

ISSN 2050-7526

ROYAL SOCIETY OF CHEMISTRY

COMMUNICATION

Ru-Shi Liu *et al.*

Synthesis of $Na_2SiF_6:Mn^{4+}$ red phosphors for white LED applications by co-precipitation

Journal of Materials Chemistry C

COMMUNICATION

View Article Online
View Journal | View Issue

Cite this: J. Mater. Chem. C, 2014, 2, 10268

Received 14th September 2014
Accepted 1st October 2014

DOI: 10.1039/c4tc02062f

www.rsc.org/MaterialsC

Synthesis of $Na_2SiF_6:Mn^{4+}$ red phosphors for white LED applications by co-precipitation†

Hoang-Duy Nguyen,‡[ab] Chun Che Lin,‡[a] Mu-Huai Fang[a] and Ru-Shi Liu*[ac]

A one-step approach to synthesize $Na_2SiF_6:Mn^{4+}$ and $K_2SiF_6:Mn^{4+}$ red phosphors by co-precipitation is reported in this paper. The phosphors were precipitated from a silicon fluoride solution with NaF and Na_2MnO_4 ($Na_2SiF_6:Mn^{4+}$ preparation) or KF and K_2MnO_4 ($K_2SiF_6:Mn^{4+}$ preparation) using H_2O_2 to reduce Mn^{7+} to Mn^{4+} at room temperature. $Na_2SiF_6:Mn^{4+}$ was also prepared through a convenient two-step route with K_2MnF_6 as a raw material. The obtained $Na_2SiF_6:Mn^{4+}$ phosphors have hexagonal structures with space group D_3^2-$P321$ and no impurity phase when they were examined *via* X-ray diffraction. Photoluminescence, photoluminescence excitation, thermal luminescence, and luminescence decay time were considered to determine the optical properties of the fluoride complexes. The prepared phosphors exhibited bright red emission under 460 nm light excitation and low-thermal quenching (~92% of the luminescent intensity at 423 K). Increasing the concentration of Mn^{4+} enhanced the luminescence intensity. A warm white light LED with high color rendering index (R_a = 86 and R9 = 61) was fabricated by employing $Na_2SiF_6:Mn^{4+}$ as red phosphors and commercial $Y_3Al_5O_{12}:Ce^{3+}$ as yellow phosphors on a blue-InGaN chip.

1. Introduction

White light-emitting diodes (WLEDs) have attracted much attention because of their energy-saving and environmentally friendly characteristics.[1,2] Most commercial WLEDs are based on the combination of blue LED chips and yellow-emitting $YAG:Ce^{3+}$ phosphors.[2–5] However, such an approach limits the application range to cool white light (correlated color temperature of 4000 K to 8000 K) and limits the color rendering index (CRI < 75)[6,7] because of the lack of red emission in the luminescence spectra. The use of rare-earth-activated sulfide,[10,11] molybdate/tungstate,[12] and nitride[13–15] red phosphors has been proposed to fabricate warm WLEDs with high color-rendering index (CRI, R_a > 80) and low correlated color temperatures (2700 K to 4000 K).[7–9] However, these materials have drawbacks. Although they possess attractive luminescence, sulfide phosphors strongly quench emission with temperature and are highly sensitive toward hydrolysis because of their rather ionic nature of binary sulfides. A high color rendering index was observed for Eu^{3+}-activated phosphors, but they have low absorption in blue or near-UV light, which can be attributed to the parity-forbidden 4f–4f transitions. Although nitride phosphors are commercially applied because of their sufficient chemical strength and efficient luminescence, their broad emission bands greatly limit the maximum achievable luminous efficacies of high-quality warm WLEDs.[9,16]

Recent studies have focused on the preparation of narrow-band red-emitting fluoride phosphors doped by manganese(IV) (Mn^{4+}) because of their good thermal stability and potential applications in solid-state light sources. The valence states of Mn (2+, 3+, 4+, 6+ and 7+) are sensitive to the synthesis temperature. Hence, the main difficulty lies in controlling the Mn valence state for synthesizing Mn^{4+}-activated fluoride complexes. Adachi *et al.* prepared a series of red fluoride phosphors, $A_2MF_6:Mn^{4+}$ (A = K, Na, Cs, or NH_4; M = Si, Ge, Zr, Sn, or Ti) and $BSiF_6:Mn^{4+}$ (B = Ba or Zn), *via* wet chemical etching of silicon wafers in aqueous HF solution with the addition of oxidizing agent $KMnO_4$ at room temperature.[17–26] The fluoride complexes have broad, intensive absorption in the long-wavelength region, which complements the electroluminescence of commercial blue LEDs, and generate highly efficient red light. However, the technique has significant drawbacks, namely, expensive pure Si wafers and metal shots used during synthesis, prolonged reaction time, tedious post-treatment, and low yield.

[a]Department of Chemistry, National Taiwan University, Taipei 106, Taiwan. E-mail: rsliu@ntu.edu.tw

[b]Institute of Applied Material Science, Vietnam Academy of Science and Technology, Hochiminh City, Vietnam

[c]Department of Mechanical Engineering and Graduate Institute of Manufacturing Technology, National Taipei University of Technology, Taipei 106, Taiwan

† Electronic supplementary information (ESI) available. See DOI: 10.1039/c4tc02062f

‡ H.-D. Nguyen and C. C. Lin contributed equally.

Convenient synthesis methods and the photoluminescence properties of fluoride phosphors have received much attention. Fluoride red phosphors – K_2TiF_6:Mn^{4+} and K_2SiF_6:Mn^{4+} prepared through a cation exchange reaction by mixing fluoride hosts with HF solution dissolved with K_2MnF_6 powders at room temperature in 20 minutes; K_2SiF_6:Mn^{4+} prepared *via* a redox reaction in HF/$KMnO_4$ solution at room temperature in 10 minutes; K_2SiF_6:Mn^{4+}, $BaTiF_6$:Mn^{4+} and $BaSiF_6$:Mn^{4+} prepared by a hydrothermal method at 120 °C in 12–20 h – have shown high emission efficiency.[27–31] However, these feasible approaches could not be applied for preparing all kinds of fluoride phosphors, Na_2SiF_6:Mn^{4+} is an example. Therefore, a simple co-precipitation method to synthesize Na_2SiF_6:Mn^{4+} and K_2SiF_6:Mn^{4+} is presented in this paper. The prepared phosphor powders, which could be used for commercial applications, exhibited efficient emission intensity, high color purity, and excellent thermal stability. Silicon oxide is easily dissolved in a concentrated HF solution. Thus, chemical co-precipitation of Na^+ and SiF_6^{4-} can be performed in HF/$NaMnO_4$ solution using H_2O_2 to efficiently reduce Mn^{7+} to Mn^{4+} at room temperature in a few minutes, which is suitable for quantifiable production because of its high yield, good repeatability, and low cost. Na_2SiF_6:Mn^{4+} was also synthesized through a two-step co-precipitation method in which K_2MnF_6, prepared from a silicon fluoride solution in the presence of $KMnO_4$ and H_2O_2, was used as a starting material. The effect of the K_2MnF_6 concentration on the luminescence intensity of Na_2SiF_6:Mn^{4+} was determined. The prepared fluoride red phosphors are potential candidates for warm WLED applications.

2. Experimental

One-step approach: Na_2SiF_6:Mn^{4+} (NSFM-1S) was synthesized through a simple one-step method (Fig. 1). Silicon fluoride solution was formed by dissolving 1.2 g SiO_2 powders in 25 mL 48% HF solution at 60 °C for 2 h. The solution was cooled to room temperature and separated from residual powder using filter paper. Solution A was formed by adding 1.84 g $NaMnO_4$·H_2O to the filtered solution. Thereafter, a saturated NaOH (1.6 g NaOH in 15 mL 48% HF) or Na_2CO_3 (1.6 g Na_2CO_3 in 15 mL 48% HF) or Na_2SO_4 (3.0 g Na_2SO_4 in 15 mL 48% HF) solution containing 1.0 mL H_2O_2 (35% to 40%) was added to solution A under vigorous stirring. The deep purple solution rapidly turned pale orange. The powder was obtained as 100 mL acetone (99.9%) was poured into the resulting solution. The powder was dried at 70 °C after washing with 20% HF solution to remove undesired products and residual chemicals, and then with ethanol several times (99.9%).

K_2SiF_6:Mn^{4+} (KSFM-1S) was also prepared following the one-step method, but $KMnO_4$ and KF, instead of $NaMnO_4$ and NaOH, were used. (The structure and luminescence properties of KSFM-1S are shown in the ESI, Fig. S3–S6.†)

Two-step approach: K_2MnF_6 was used as a raw material for the two-step synthesis of Na_2SiF_6:Mn^{4+} (NSFM-2S) phosphors (Fig. 2). For K_2MnF_6 preparation, a mixture, which consisted of 9.0 g KHF_2 and 0.45 g $KMnO_4$, was dissolved in a 30 mL solution of 48% HF. Then, 0.3 mL H_2O_2 (35% to 40%) was added to the solution using a dropper. The deep purple solution gradually turned yellow, and a yellow precipitate was obtained. The powder was washed with acetone several times and dried at 70 °C for 2 h. The K_2MnF_6 product was identified *via* X-ray powder diffraction (XRD; D2PHASER:Cu-Kα radiation, Bruker AXS, Germany; ESI Fig. S7†) before it was used for Na_2SiF_6:Mn^{4+} synthesis. The prepared K_2MnF_6 powder (0.05 g to 0.30 g) was dissolved in the silicon fluoride solution (1.2 g SiO_2 and 25 mL 48% HF) while stirring. Then, 4.2 g Na_2SO_4 was added slowly to the solution for 3 min to 5 min while stirring for 15 min. Yellow powder was obtained and washed with 20% HF solution, washed twice with ethanol (99.9%), and dried at 70 °C for 6 h.

The prepared NSFM-1S and NSFM-2S samples show a uniform pale yellow tint under warm light illumination (Fig. 1a and 2a), and generate bright red light under 365 nm illumination (Fig. 1b and 2b). The scanning electron micrographs of Na_2SiF_6:Mn^{4+} red phosphors show Na_2SiF_6 near round-like crystals prepared *via* both methods (Fig. 1c and 2c). The particle size was primarily in the range of 1 μm to 5 μm for NSFM-1S and 5 μm to 10 μm for NSFM-2S.

The purity and structure of the obtained phosphors were examined *via* XRD. A scanning electron microscope (JEOL JSM-6700F, Japan) was used to characterize the morphology of the fluoride materials. A FluoroMax-3 spectrophotometer (HORIBA, Japan) equipped with a 150 W Xe lamp was used to measure the RT excitation and emission spectra. For temperature-dependent experiments at 303–573 K, the samples were placed in a small platinum hold with its temperature controlled by a heating THMS-600 device (Linkam Scientific Instruments Ltd., UK). Light was radiated using a Hamamatsu R928 photo-multiplier tube.

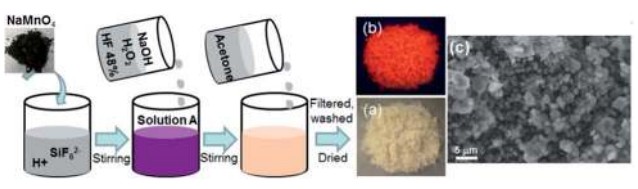

Fig. 1 Synthesis of Na_2SiF_6:Mn^{4+} red phosphors *via* a one-step method, and digital images of Na_2SiF_6:Mn^{4+} under (a) warm room light and (b) UV light (λ_{ex} = 365 nm) excitation; (c) scanning electron micrographs of NSFM-1S.

Fig. 2 Synthesis of Na_2SiF_6:Mn^{4+} red phosphors *via* a two-step method, and digital images of Na_2SiF_6:Mn^{4+} under (a) warm light and (b) UV light (λ_{ex} = 365 nm) excitation; (c) scanning electron micrographs of NSFM-2S.

The commercial YAG:Ce^{3+} yellow phosphors, Na_2SiF_6:Mn^{4+} red phosphors and blue chips (455 nm, 250 mW, 350 mA, APT Electronics Ltd., China) were used to fabricate WLEDs. The phosphors were mixed with silicone resin (Dow Corning OE-6630 A and B) thoroughly. The obtained phosphor–silicone mixture was coated on the surface of the LED chips. The photoelectric properties of the fabricated devices were measured using an integrating sphere spectroradiometer system (PMS-80, Everfine Photo-EINFO Co. Ltd., China). The LEDs were operated at 2.0 V with a current of 200 mA.

3. Results and discussion

Synthesis strategy: H_2O_2 was used during preparation to reduce the reaction time. The co-precipitation of silicon fluoride with NaF in HF/$NaMnO_4$ solution in the presence of H_2O_2 is represented as follows:

$$NaOH + HF \rightarrow NaF + H_2O$$

$$(2-2x)SiO_2 + 2xNaMnO_4 + (4-2x)NaF + (8+2x)HF + (2-x)H_2O_2 \rightarrow 2Na_2Si_{1-x}Mn_xF_6 + 6H_2O + (1+x)O_2\uparrow$$

The amount of K_2MnF_6 in the two-step approach should not exceed 0.30 g to prevent undesired K_2SiF_6 precipitation. Given that the solubility of K_2SiF_6 ($S_{K_2SiF_6}$) in 48% HF solution is 0.146 M,[32] the precipitation will occur as

$$[K^+]^2 \times [SiF_2{}^{2-}] \geqq 4 \times (S_{K_2SiF_6})^3 \sim 1.24 \times 10^{-2}.$$

The silicon fluoride solution used in the preparation process had a concentration of 0.8 M. Therefore, the K^+ concentration in the prepared solution should be lower than 0.124 M, and the K_2MnF_6 concentration should not be higher than 0.062 M (~0.38 g K_2MnF_6 in 25 mL 48% HF solution).

Na_2SiF_6:Mn^{4+} phosphors prepared by different methods have diverse XRD patterns and crystal structures (Fig. 3a). All diffracted peaks can be indexed to the space group $D_3{}^2$-$P321$ of hexagonal Na_2SiF_6 (JCPDS no. 33-1280). Neither K_2SiF_6 nor secondary phases were identified, indicating that all prepared samples have a single phase, Na_2SiF_6:Mn^{4+}. The crystal structure of Na_2SiF_6 viewed from the [110] direction is shown in Fig. 3b. Each Si^{4+} is surrounded by six F^- to form a regular $SiF_6{}^{2-}$ octahedron. Na^+ is at the center of 12 neighboring F forming a nearly regular polyhedron.

The photoluminescence excitation (PLE) and photoluminescence (PL) spectra of Na_2SiF_6:Mn^{4+} red phosphors were recorded at room temperature (Fig. 4a). The emission at 620 nm (λ_{em} = 620 nm) was monitored. The excitation spectrum exhibited two broad bands with peaks at ~460 and ~360 nm, mainly because of the spin-allowed transitions of $^4A_{2g} \rightarrow {}^4T_{1g}$ and $^4A_{2g} \rightarrow {}^4T_{2g}$, respectively. The sharp red emission lines from 600 nm to 650 nm originated from the spin-forbidden $^2E_g \rightarrow {}^4A_{2g}$ transitions.[27,33] The seven main peaks in the emission band, at ~594, 605, 609, 618, 627, 631, and 643 nm, are due to transitions of the ν_3 (t_{1u}), ν_4 (t_{1u}), ν_6 (t_{2u}), zero phonon line (ZPL), ν_6 (t_{2u}), ν_4 (t_{1u}), and ν_3 (t_{1u}) vibronic modes, respectively, similar to that of Na_2SiF_6:Mn^{4+} prepared by wet chemical etching of a Si wafer.[18,19] ZPL emission is clearly observed in the PL spectra of the Na_2SiF_6:Mn^{4+} hexagonal phase at room temperature, but hardly observed in those of the K_2SiF_6:Mn^{4+} cubic phase (Fig. 4b). The ZPL emission intensity is dependent on the local symmetry of the Mn^{4+} ion surroundings. A Mn^{4+} activated material with lower crystal symmetry is expected to show higher ZPL emission intensity.[19]

No K_2SiF_6:Mn^{4+} phase could be found in Na_2SiF_6:Mn^{4+} samples prepared by the two-step method. The luminescence intensity of Na_2SiF_6:Mn^{4+} increased along with the concentration of K_2MnF_6 (Fig. 4c). The red emission (627 nm) intensity of

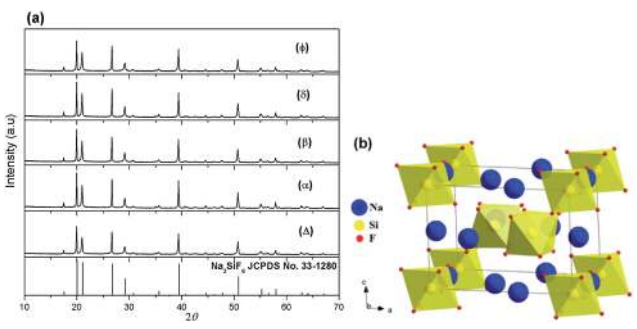

Fig. 3 (a) XRD patterns of (Δ) NSFM-1S, and NSFM-2S using (α) 0.008, (β) 0.016, (δ) 0.032, and (ϕ) 0.048 M of K_2MnF_6; (b) crystal structure of Na_2SiF_6:Mn^{4+}.

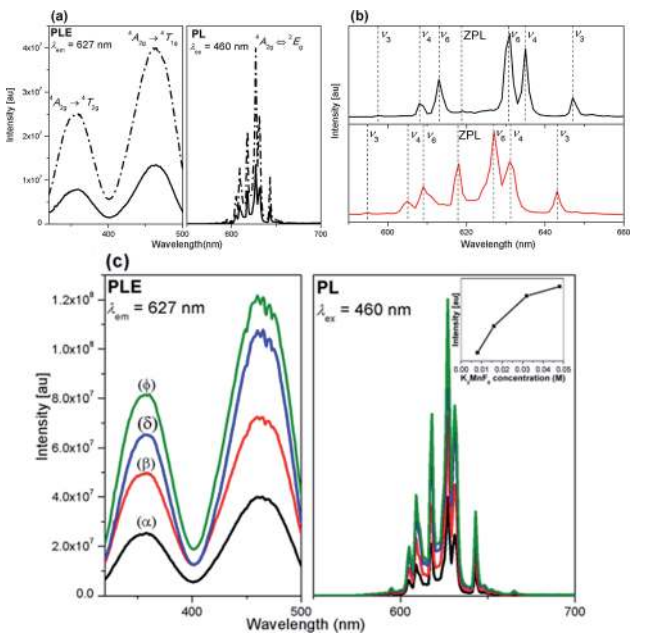

Fig. 4 (a) PLE and PL spectra of NSFM-1S (solid line) and NSFM-2S (dash-dotted line); (b) PL spectra of KSFM-1S (black line) and NSFM-2S (red line); (c) PLE and PL spectra of NSFM-2S using (α) 0.008, (β) 0.016, (δ) 0.032 and (ϕ) 0.048 M of K_2MnF_6; the inset image shows 627 nm emission intensity as a function of K_2MnF_6 concentration under 460 nm light excitation.

$Na_2SiF_6:Mn^{4+}$ under 460 nm light excitation is a function of K_2MnF_6 concentration, and the optimum concentration of K_2MnF_6 is 0.048 M (inset in Fig. 4c). A higher concentration of K_2MnF_6 may lead to the formation of undesired potassium compounds.

Room temperature PL decay characteristics of the emitting state ^2E_g in the prepared phosphors are shown (Fig. 5). The PL decay time was determined based on a single exponential fit. The PL lifetimes of 4.8, 5.8, and 7.4 ms were found for NSFM-1S, NSFM-2S, and KSMF-1S, respectively. The results complement the $Na_2SiF_6:Mn^{4+}$ and $K_2SiF_6:Mn^{4+}$ phosphors prepared by Adachi *et al.*'s etching method.[17–19]

The temperature-dependent emission spectra of $Na_2SiF_6:Mn^{4+}$ phosphors under 460 nm light excitation are also presented (Fig. 6a). On increasing the temperature from 303 K to 573 K, emission lines all became broader and red shifted because of the increased absorbed photons and enhanced vibration transition coupling associated with the vibration modes of MnF_6^{2-} octahedra. The temperature-dependent behavior of integrated PL intensity (I_{PL}/I_{PL303}) (Fig. 6b) showed considerable stability for $Na_2SiF_6:Mn^{4+}$ red phosphors in the temperature range of 303 K to 423 K. At 432 K, the relative PL intensity of the sample remained at 92% of that at 303 K, clearly showing better thermal stability than the widely used YAG:Ce phosphors[34] (88% at 423 K). Non-radiative transition probability increased with temperature and integrated PL intensity showed thermal quenching, which can be fitted by $I_T/I_0 = [1 + D\exp(-E_a/kT)]^{-1}$, where I_0 is the intensity at $T = 0$ K, and D and activation energy E_a are refined variables. The activation energy obtained for $Na_2SiF_6:Mn^{4+}$ red phosphors was 0.62 eV, three times higher than that of nitride compounds[35] (~0.23 eV), confirming the excellent thermal stability of the subject phosphors.

The performance of WLEDs fabricated by combining blue InGaN chips, commercial $Y_3Al_5O_{12}:Ce^{3+}$ yellow phosphors and NSFM-2S red phosphors is evaluated for commercial applications. The sharp emission lines of Mn^{4+} in the Na_2SiF_6 lattice are observed in the electroluminescence spectra of the WLED (Fig. 6c). A luminous efficacy of 77.6 lm W^{-1}, CRI of 86 and R9 = 61 for the WLED is obtained under a drive current of 200 mA (inset image). Chromaticity coordinates (0.3126 and 0.2951) laid near the black body locus in Commission Internationale de

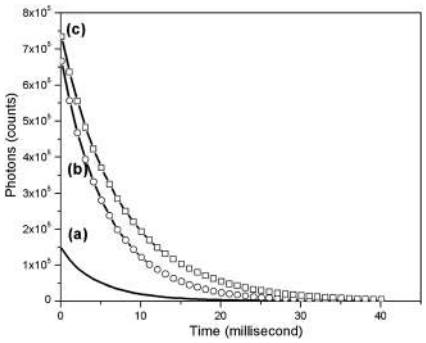

Fig. 5 PL decay curves of (a) NSFM-1S, (b) NSFM-2S, and (c) KSF-1S at 300 K.

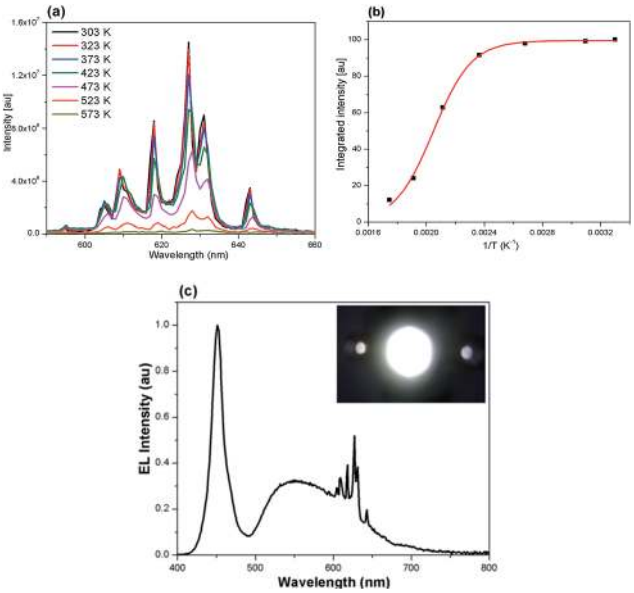

Fig. 6 (a) Temperature-dependent emission spectra of $Na_2SiF_6:Mn^{4+}$; (b) integrated red PL intensity as a function of temperature (303 K to 573 K) for NSFM-2S. The solid line represents the fitting result with the expression of $I_T/I_0 = [1 + D\exp(-E_a/kT)]^{-1}$ for NSFM-2S; (c) luminescence spectra of the white-LEDs used $Na_2SiF_6:Mn^{4+}$ red phosphors; the inset image shows bright white-light emitted from the fabricated WLED.

l'Éclairage (CIE) 1931 color spaces and a color temperature of 6875 K was observed for the fabricated WLEDs (Fig. S8†). The thermal stability and package results indicate that the $Na_2SiF_6:Mn^{4+}$ red phosphors are promising candidates for improving the color reproducibility of the current commercial white-LEDs.

4. Conclusions

In conclusion, red fluoride phosphors $Na_2SiF_6:Mn^{4+}$ and $K_2SiF_6:Mn^{4+}$ were synthesized using simple co-precipitation routes. NSFM-1S and NSFM-2S had a micrometer-sized hexagonal structure. No impurities or other fluoride phases were detected in the NSFM-2S samples. The prepared phosphors had strong blue-light absorption and intense narrow-band red-emission. The luminescence intensity of NSFM-2S phosphors significantly increased when the Mn^{4+} content was increased. The NSFM-2S phosphors exhibited excellent thermal stability with integrated PL intensity over 90% at 423 K. A significant improvement in CRI (86) of the WLED fabricated using $Na_2SiF_6:Mn^{4+}$ red phosphors was observed. Efficient red luminescence under blue light excitation, low-thermal quenching, and a simple synthesis process make $Na_2SiF_6:Mn^{4+}$ a potential candidate for improving the color reproducibility of WLEDs.

Acknowledgements

The authors would like to thank the National Science Council of the Ministry of Science and Technology of Taiwan (Contract no.

MOST 101-2113-M-002-014-MY3) for the financial support of this study.

References

1 M. H. Chang, D. Das, P. V. Varde and M. Pecht, *Microelectron. Reliab.*, 2012, **52**, 762–782.
2 I. Ahemen, K. DeDilip and A. N. Amah, *Appl. Phys. Res.*, 2014, **6**, 95–108.
3 R. Zhang, H. Lin, Y. Yu, D. Chen, J. Xu and Y. Wang, *Laser Photonics Rev.*, 2014, **8**, 158–164.
4 H. Shi, C. Zhu, J. Huang, J. Chen, D. Chen, W. Wang, F. Wang, Y. Cao and X. Yuan, *Opt. Mater. Express*, 2014, **4**, 649–655.
5 C. C. Lin and R. S. Liu, *J. Phys. Chem. Lett.*, 2011, **2**, 1268–1277.
6 P. Schlotter, R. Schmidt and J. Schneider, *Appl. Phys. A*, 1997, **64**, 417–418.
7 P. Pust, V. Weiler, C. Hecht, A. Tücks, A. S. Wochnik, A.-K. Hen, D. Wiechert, C. Scheu, P. J. Schmidt and W. Schnick, *Nat. Mater.*, 2014, **13**, 891–896.
8 M. R. Krames, O. B. Shchekin, R. Mueller-Mach, G. O. Mueller, L. Zhou, G. Harbers and M. G. Crafor, *J. Disp. Technol.*, 2007, **3**, 160–175.
9 P. F. Smet, A. B. Parmentier and D. Poelman, *J. Electrochem. Soc.*, 2011, **158**, R37–R54.
10 D. Poelman, J. E. V. Haecke and P. F. Smet, *J. Mater. Sci.: Mater. Electron.*, 2009, **20**, S134–S138.
11 R. Mueller-Mach and G. O. Mueller, *Proc. SPIE*, 2000, **3938**, 30–41.
12 P. S. Dutta and A. Khanna, *ECS J. Solid State Sci. Technol.*, 2013, **2**, R3153–R3167.
13 R.-J. Xie, N. Hirosaki, K. Sakuma and N. Kimura, *J. Phys. D: Appl. Phys.*, 2008, **41**, 144013.
14 H. Nersisyan, H. I. Won and C. W. Won, *Chem. Commun.*, 2011, **47**, 11897–11899.
15 K. Uheda, N. Hirosaki, Y. Yamamoto, A. Naito, T. Nakajima and H. Yamamoto, *Electrochem. Solid-State Lett.*, 2006, **9**, H22–H25.
16 N. C. George, K. A. Denault and R. Seshadri, *Annu. Rev. Mater. Res.*, 2013, **43**, 481–501.
17 T. Takahashi and S. Adachi, *J. Electrochem. Soc.*, 2008, **155**, E183–E188.
18 S. Adachi, H. Abe, R. Kasa and T. Arai, *J. Electrochem. Soc.*, 2012, **159**, J34–J37.
19 Y. K. Xu and S. Adachi, *J. Appl. Phys.*, 2009, **105**, 013525.
20 Y. Arai and S. Adachi, *J. Lumin.*, 2011, **131**, 2652–2660.
21 R. Kasa and S. Adachi, *J. Appl. Phys.*, 2012, **112**, 013506.
22 Y. Arai, T. Takahashi and S. Adachi, *Opt. Mater.*, 2010, **32**, 1095–1101.
23 Y. K. Xu and S. Adachi, *J. Electrochem. Soc.*, 2011, **158**, J58–J65.
24 Y. K. Xu and S. Adachi, *J. Electrochem. Soc.*, 2012, **159**, E11–E17.
25 D. Sekiguchi, J. Nara and S. Adachi, *J. Appl. Phys.*, 2013, **113**, 183516.
26 R. Hoshino and S. Adachi, *J. Appl. Phys.*, 2013, **114**, 213502.
27 H. Zhu, C. C. Lin, W. Luo, S. Shu, Z. Liu, Y. Liu, J. Kong, E. Ma, Y. Cao, R. S. Liu and X. Chen, *Nat. Commun.*, 2014, **5**, 4312 1.
28 C. Liao, R. Cao, Z. Ma, Y. Li, G. Dong, K. N. Sharafudeen and J. Qiu, *J. Am. Ceram. Soc.*, 2013, **96**, 3552–3556.
29 X. Jiang, Y. Pan, S. Huang, X. Chen, J. Wang and G. Liu, *J. Mater. Chem. C*, 2014, **2**, 2301–2306.
30 X. Jiang, Z. Chen, S. Huang, J. Wang and Y. Pan, *Dalton Trans.*, 2014, **43**, 9414–9418.
31 L. Lv, X. Jiang, S. Huang, X. Chen and Y. Pan, *J. Mater. Chem. C*, 2014, **2**, 3879–3884.
32 J. Frayret, A. Castetbon, G. Trouve and M. Potin-Gautier, *Chem. Phys. Lett.*, 2006, **427**, 356–364.
33 Y. Tanabe and S. Sugano, *J. Phys. Soc. Jpn.*, 1954, **9**, 753–766.
34 Q. Shao, H. Li, Y. Dong, J. Jiang, C. Liang and J. He, *J. Alloys Compd.*, 2010, **498**, 199–202.
35 S. S. Wang, W. T. Chen, Y. Li, J. Wang, H. S. Sheu and R. S. Liu, *J. Am. Chem. Soc.*, 2013, **135**, 12504–12507.

